REPORT DOCUMENTATION PAGE

Form Approved
OMB No. 0704-0188

Public reporting burden for this collection of information is estimated to average 1 hour per response, including the time for reviewing instructions, searching existing data sources, gathering and maintaining the data needed, and completing and reviewing the collection of information. Send comments regarding this burden estimate or any other aspect of this collection of information, including suggestions for reducing this burden, to Washington Headquarters Services, Directorate for Information Operations and Reports, 1215 Jefferson Davis Highway, Suite 1204, Arlington, VA 22202-4302, and to the Office of Management and Budget, Paperwork Reduction Project (0704-0188), Washington, DC 20503.

1. AGENCY USE ONLY (Leave blank)	2. REPORT DATE	3. REPORT TYPE AND DATES COVERED
	Jan 95	Technical

4. TITLE AND SUBTITLE

Graphical Shape Templates for Deformable Model Registration with Applications to MRI Brain Scans

5. FUNDING NUMBERS

DAAL03-92-G-0322

6. AUTHOR(S)

Yali Amit

7. PERFORMING ORGANIZATION NAME(S) AND ADDRESS(ES)

University of Chicago
Chicago, IL 60637

DTIC ELECTE FEB 23 1995 S D G

8. PERFORMING ORGANIZATION REPORT NUMBER

9. SPONSORING/MONITORING AGENCY NAME(S) AND ADDRESS(ES)

U.S. Army Research Office
P.O. Box 12211
Research Triangle Park, NC 27709-2211

10. SPONSORING/MONITORING AGENCY REPORT NUMBER

ARO 30167.8-MA

11. SUPPLEMENTARY NOTES

The views, opinions and/or findings contained in this report are those of the author(s) and should not be construed as an official Department of the Army position, policy, or decision, unless so designated by other documentation.

12a. DISTRIBUTION/AVAILABILITY STATEMENT

Approved for public release; distribution unlimited.

12b. DISTRIBUTION CODE

13. ABSTRACT (Maximum 200 words)

A new method of template matching is proposed using graphical templates. A graph of landmarks is chosen in the template image. All possible candidates for these landmarks are found in the data image using robust relational local operators. A dynamic programming algorithm on decomposable subgraphs of the template graph finds the optimal match to a subset of the candidate points in *polynomial time*. This combination of local operators to describe points of interest/landmarks and a graph

DTIC QUALITY INSPECTED CONT'D ON REVERSE SIDE

19950216 058

14. SUBJECT TERMS	15. NUMBER OF PAGES
Shape and object representation, Medical computer vision, graphical templates	20
	16. PRICE CODE

17. SECURITY CLASSIFICATION OF REPORT	18. SECURITY CLASSIFICATION OF THIS PAGE	19. SECURITY CLASSIFICATION OF ABSTRACT	20. LIMITATION OF ABSTRACT
UNCLASSIFIED	UNCLASSIFIED	UNCLASSIFIED	UL

DISCLAIMER NOTICE

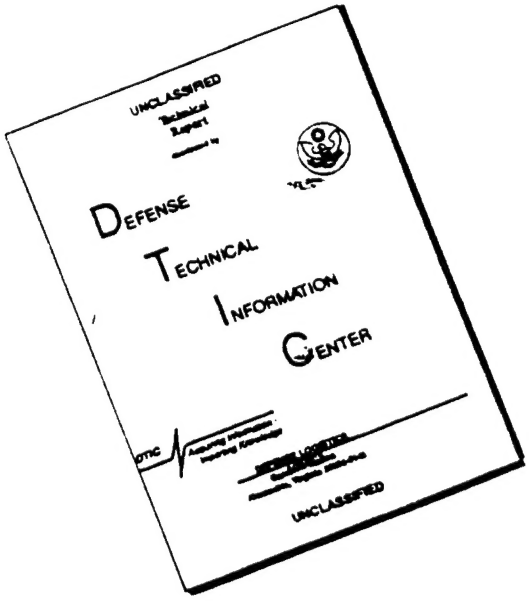

THIS DOCUMENT IS BEST QUALITY AVAILABLE. THE COPY FURNISHED TO DTIC CONTAINED A SIGNIFICANT NUMBER OF PAGES WHICH DO NOT REPRODUCE LEGIBLY.

to describe their geometric orientation in the plane, yields fast and precise matches of the model to the data, with no initialization required. In addition it provides a generic toolbox for modeling shape in a variety of applications. This methodology is applied in the context of T2 weighted MR images of the brain.

GRAPHICAL SHAPE TEMPLATES FOR DEFORMABLE MODEL REGISTRATION WITH APPLICATIONS TO MRI BRAIN SCANS

Yali Amit

TECHNICAL REPORT NUMBER 402

Department of Statistics

University of Chicago

Chicago, IL 60637

Key words: Shape and object representation, Medical computer vision, graphical templates.

* Research supported in part by ARO DAAL03-92-G-0322.

Accesion For

NTIS CRA&I [X]
DTIC TAB [ ]
Unannounced [ ]
Justification .....

By .....
Distribution /

Availability Codes

Dist	Avail and / or Special
A-1	

ABSTRACT

A new method of template matching is proposed using graphical templates. A graph of landmarks is chosen in the template image. All possible candidates for these landmarks are found in the data image using robust relational local operators. A dynamic programming algorithm on decomposable subgraphs of the template graph finds the optimal match to a subset of the candidate points in *polynomial time*. This combination of local operators to describe points of interest/landmarks and a graph to describe their geometric orientation in the plane, yields fast and precise matches of the model to the data, with no initialization required. In addition it provides a generic toolbox for modeling shape in a variety of applications. This methodology is applied in the context of T2 weighted MR images of the brain.

§1 Introduction

The main premise of this paper is that recognition and registration can be achieved through graphical models describing the *global planar arrangement of local image features or landmarks.* The local features are defined through very robust and crude local operators describing local pixel intensity topographies. They are not meant to identify any complex components with great accuracy. It is the planar configuration of these features, described in terms of a graph, which singles the true positives from the many false positives which light up for these operators.

Model registration is achieved by creating a graph (manually at this point) of triangles describing the global arrangement of the features, and then using dynamic programming on decomposable subgraphs to find the optimal match to the large collection of feature candidates which light up in the image. These methods are applied to continuously varying objects appearing in medical imaging. In this paper we present the specific case of MRI brain scans. In Amit and Kong (1993) the method was applied to hand xrays.

Using similar ingredients in Amit and Geman (1994) we describe an object recognition algorithm, implemented in the context of handwritten character recognition. Decision trees are grown, where the questions at the nodes involve incrementing graphs of binary relations between landmarks. The binary relations involve the relative orientation of the two landmarks. At each node in the tree more complex and informative questions are constructed using questions from previous nodes which were answered in the affirmative. The terminal nodes of these trees may in the future provide graphical shape models for the corresponding classes.

The problem of model registration in medical imaging is becoming of growing interest. First it provides an automatic means of identifying the various components

of the object in the image (figure 5), and in some cases of segmenting the image. Secondly it provides a means of studying the variability in the family, classifying subgroups and identifying abnormalities. Thirdly it can provide a means for coding or data compression. It is also related to issues of data fusion.

The most extensively studied models come under the general title of elastic matching.

Elastic matching versus landmark matching

Grenander (1970) introduced the idea of elastic deformations of one and two dimensional templates. These ideas were implemented in a Bayesian framework using spectral representations of the planar maps in Amit *et. al.* (1991) for hand xrays and in Miller *et. al.* (1993) for MRI images of the brain. Similar ideas were proposed by Bajcsy and Kovacic (1989) for MRI brain images, using techniques developed in the optical flow and image sequence analysis literature. Horn and Schunck (1980), Huang and Tsai (1981) and Nagel (1983), Terzopoulos (1988). A comparison of these methods both from the point of view of the optimization problem being posed and the numerical techniques can be found in Amit (1994). One dimensional elastic models have also been extensively studied see Grenander *et. al* (1991), and Kass *et. al.* (1987).

There are several limitations to these elastic models. First the matching criterion seeks to minimize the mean square over all pixels of the difference between the intensity of the deformed template and that of the data image. On one hand this is a very well defined criterion however it does not ensure that specific points of interest or landmarks be matched with great precision. This later criterion is very precisely defined for the human eye but very hard to formulate in mathemat-

ical terms. Second the deformations being used are generic or non-parametric in nature and do not depend on the specific family of objects. Third, because of the inherent non-linearity of the problem, and the fact that the deformations are high dimensional, the computational tools for calculating the match must use relaxation techniques which run the risk of converging to a local minimum which corresponds to a poor match. This is a serious problem in the one dimensional elastic algorithms.

These issues point to three categories which must be addressed *simultaneously* and in an integrated manner in any approach to the template matching problem. The data term which drives the matching. The model and its variability. The computational tools and their limitations.

The principal tool in the method described here is a graphical model of landmark points which describes their planar arrangement, together with local operators which identify candidates for the various landmarks in the data image. This is essentially a new approach to the general program outlined in Haralick and Shapiro (1993, 16.1.2). Namely *image features* are defined and then correspondence is obtained through a *consistency model*, which is optimized through an efficient algorithm consisting of dynamic programming on decomposable subgraphs of the original model.

Thus more emphasis is put on the precise matching of landmarks, see Bookstein (1991), local features or points of interest (see Haralick and Shapiro (1993)). These landmarks are both important for understanding and analyzing the image and can be identified using various local operators which employ more information than individual pixel intensity. Moreover modeling the variability in terms of the relative locations of the landmarks yields a more specific and lower dimensional description of the variability within a certain family of objects.

From graph matching to planar maps: Once the graph has been matched to the data it is possible to create a *planar* map through interpolation as in Bookstein (1991). Furthermore this interpolated map can serve as an initial point for the elastic matching algorithms where the correct match of the landmarks is ensured.

From graph matching to component identification: Given the location of various components of interest relative to the landmarks, these can be automatically identified once the graph has been matched. For example the various anatomies present in the T2 weighted MRI brain scan in figure 5 were identified automatically using the match displayed in figure 4.

Ultimately, for each specific anatomy or image family we will have a graph which will be automatically matched to any incoming data image, yielding an automatic identification of the various components. This method can be thought of as a generic *toolbox for modeling shape.*

In section 2 some of the details of the graph matching algorithm are described together with some of the experiments.

§2 The graph matching algorithm

A template image is chosen from the family for the construction of the local operators and graphical model. For the purpose of obtaining planar maps and image compression this template image is considered as part of the model, together with the graph of landmarks.

2.1 The local operators

A collection of landmarks is chosen in the template image (figure 1) and a local operator is chosen for each landmark. The local operators are designed to be

robust, and hence crude, descriptions of the local topography of the pixel intensity function in the neighborhood of the landmark.

A certain size neighborhood is chosen, say $m \times n$, together with an array L of 1-s, -1-s and 0-s of those dimensions. The *sign* of the difference between the intensity at a given pixel i, j, and the intensity at each of the pixels in its $m \times n$ neighborhood is calculated, to yield an array $A^{(i,j)}$ of 1-s and -1-s, at pixel i, j. If the percentage of matched 1-s and -1-s between L and $A^{(i,j)}$ is above a prescribed threshold the pixel is considered a candidate for the corresponding landmark. The 0-s region in L represents a region where the results of the $A^{(i,j)}$ are ignored. The simplest example is L_1 all 1-s, and L_{-1} all 0-s. This corresponds to a local maximum operator. The reverse corresponds to a local minimum operator. The pixels corresponding to a certain local operator typically occur in clusters. These were identified and the average location calculated.

In the experiments described below on MRI brain scans the operators for the eight landmarks were obtained by pointing to the eight points in the template image, extracting an 11×11 neighborhood and calculating the matrix of signs of differences with respect to the middle pixel. Below is an example of the operator used to identify candidates for landmark no. 1 in figure 1.

$$\begin{pmatrix}
1 & 1 & 1 & 1 & 1 & 1 & 1 & 1 & 1 & 1 & 1 \\
1 & 1 & 1 & 1 & 1 & 1 & 1 & 1 & 1 & 1 & 1 \\
-1 & -1 & -1 & 1 & 1 & 1 & 1 & 1 & 1 & -1 & -1 \\
-1 & -1 & -1 & -1 & 1 & 1 & 1 & 1 & -1 & -1 & -1 \\
-1 & -1 & -1 & -1 & -1 & 1 & 1 & -1 & -1 & -1 & -1 \\
-1 & -1 & -1 & -1 & -1 & 1 & -1 & -1 & -1 & -1 & -1 \\
-1 & -1 & -1 & -1 & -1 & -1 & -1 & -1 & -1 & -1 & -1 \\
-1 & -1 & -1 & -1 & -1 & -1 & -1 & -1 & -1 & -1 & -1 \\
-1 & -1 & -1 & -1 & -1 & -1 & -1 & -1 & -1 & -1 & -1 \\
-1 & -1 & -1 & -1 & -1 & -1 & -1 & -1 & -1 & -1 & -1 \\
-1 & -1 & -1 & -1 & -1 & -1 & -1 & -1 & -1 & -1 & -1
\end{pmatrix}$$

The left panel in figure 2 displays as circles the candidates for this operator using a threshold of .75 The right panel displays the outcome with a threshold of .8. False negatives are to be avoided at all costs because then there will not be a match in the image for a specific landmark. This is done by lowering the thresholds and increasing the number of false positives. Dealing with these is the role of the graphical model, which provides constraints on the planar arrangement of the landmarks. Of course too many false positives will lead to erroneous matches.

2.2 Decomposable graphs for matching

In figure 1 the eight landmarks chosen in an MRI scan of the brain are displayed.

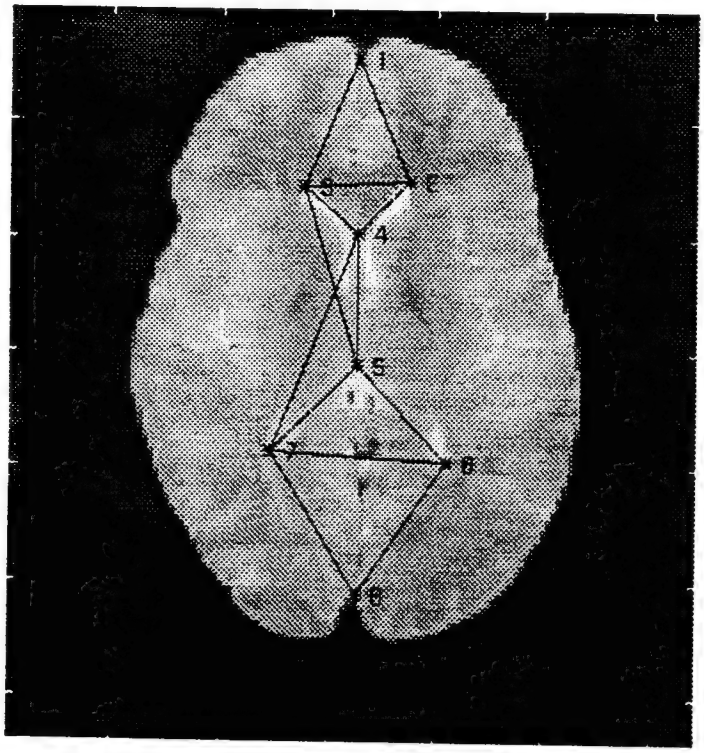

The landmarks and the graph in the template image

FIGURE 1.

Typically the same local operator will be used for several landmarks, and many

more candidates will be found in the data image, than landmarks associated with that operator in the model, see figure 2.

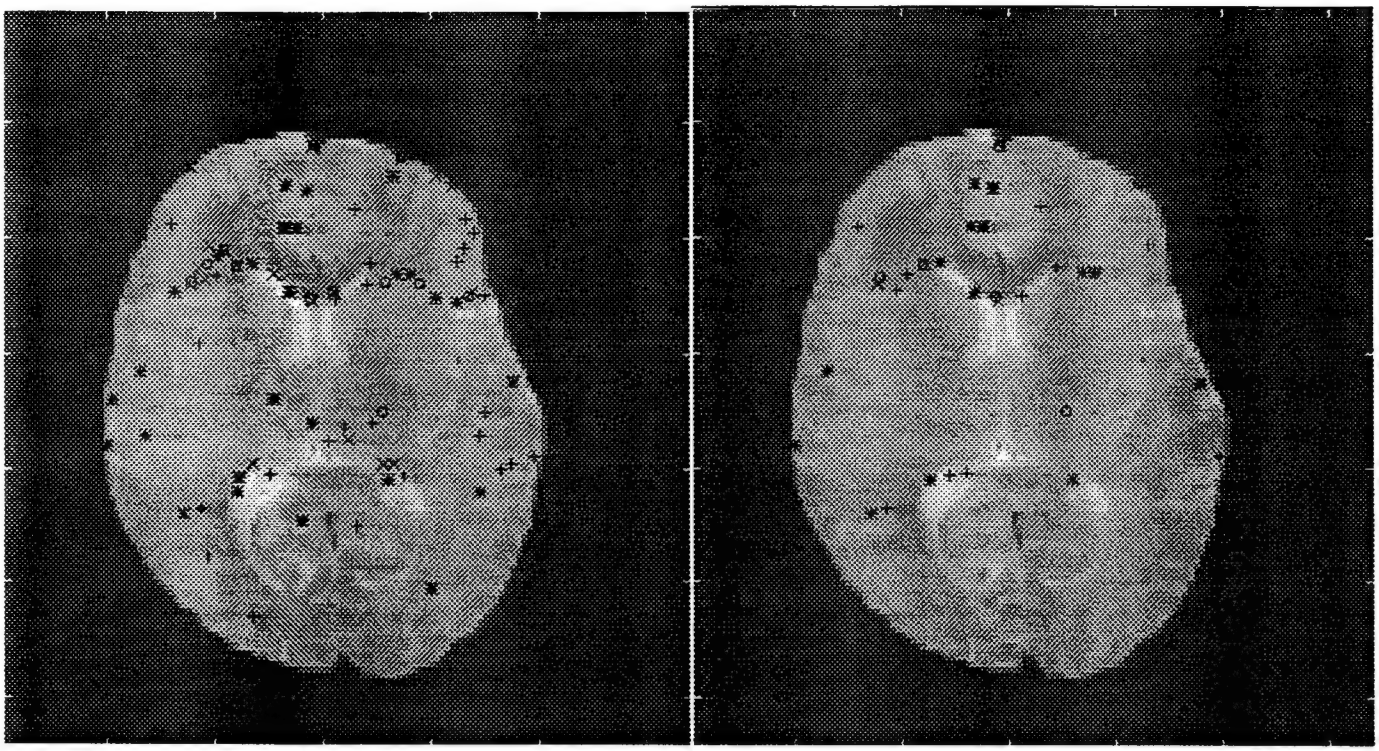

Candidates for the first 4 landmarks found in the data. $1 - o, 2 - +, 3 - *, 4 - x$.
Left panel: threshold of .75. Right panel: threshold of .8

FIGURE 2.

To find the correct match of the landmarks in the model to the candidate pixels in the image it is necessary to introduce constraints on the relative locations of the landmarks in the plane. This can be done by defining a collection of triangles between triples of landmarks identified on the template image. *At present this is done manually by the user.* See figure 1. A cost function is associated with each such triangle which penalizes its shape deviation from the corresponding triangle in the template image. The total cost function is the sum of the cost functions over all the triangles in the model. The collection of triangles can also be expressed as a colored graph, where the nodes are the landmarks, the color or type of a node is

given by the type of local operator used to find its candidates. The edges in the graph exist between each two landmarks which belong to a triangle. This graph is called the template graph. In this context the deformable template is not an image but a graph model. It is important to note that these constraints need not be *local*, indeed they could involve far apart landmarks. This is in contrast to the implicit constraints used in the elasticity models which essentially penalize large changes in the local lattice elements.

Finding the optimal match then reduces to an *inexact consistent-labeling problem*, (see Haralick and Shapiro (1993, Chapter 17), which is generically exponential in complexity. However if the template graph is chosen so as to be decomposable, it is possible to find the optimal match in *polynomial time* using dynamic programming on the graph, see for example Rose *et. al.* (1976). Decomposability in the present context means that there exists an order in which the triangles of the graph can be successively eliminated, such that each triangle in its turn has a free vertex contained in no other triangle. When the free vertex and the two edges emanating from it are removed, one of the vertices of the next triangle in the order is freed and so on.

Dynamic programming on the graph

The graph displayed in figure 1 is decomposable, and the order of elimination coincides with the index number of the landmark type. Let $v_i, i = 1.....8$ denote the vertices in the graph, L_i the corresponding local operator, and d_α denote candidate points found in a data image. For each triangle i, j, k in the graph let $\phi_{ijk}(d_{\alpha_i}, d_{\alpha_j}, d_{\alpha_k})$ denote the cost incurred by matching v_i to d_{α_i}, v_j to d_{α_j} and v_k to d_{α_k}. Obviously d_{α_i} was identified with the operator L_i etc. The cost of a full

match is simply

$$\sum_{(i,j,k)\in\mathcal{C}} \varphi_{ijk}(d_{\alpha_i}, d_{\alpha_j}, d_{\alpha_k}).$$

where $\mathcal{C}$ is the collection of triangles in the graph.

Dynamic programming in this context is implemented as follows. For each possible match $d_{\alpha_2}, d_{\alpha_3}$ for vertices v_2, v_3 find the point d_{α_1} which minimizes

$$\phi_{123}(d_{\alpha_1}, d_{\alpha_2}, d_{\alpha_3}),$$

call the minimizing index $\alpha_1(\alpha_2, \alpha_3)$ and the associated cost $c_{123}(\alpha_2, \alpha_3)$. Store these two for each pair (α_2, α_3). Now for each possible match $d_{\alpha_3}, d_{\alpha_4}$ find the point d_{α_2} which minimizes

$$\varphi_{234}(d_{\alpha_2}, d_{\alpha_3}, d_{\alpha_4}) + c_{123}(\alpha_2, \alpha_3).$$

Note that the second term is already stored in memory. Again call the minimizing point $\alpha_2(\alpha_3, \alpha_4)$ and the associated cost $c_{234}(\alpha_3, \alpha_4)$, and so on until the best d_{α_6} is found for every pair of $d_{\alpha_7}, d_{\alpha_8}$ with the updated cost function

$$c_{678}(\alpha_7, \alpha_8) = \phi_{678}(d_{\alpha_6}, d_{\alpha_7}, d_{\alpha_8}) + c_{567}(\alpha_6, \alpha_7).$$

The optimal pair α_7^*, α_8^* is chosen, α_6^* is taken to be the already stored $\alpha_6(\alpha_7^*, \alpha_8^*)$, for α_5^* take $\alpha_5(\alpha_6^*, \alpha_7^*)$ and so on, until the entire optimal match $\alpha_1^*, \ldots, \alpha_8^*$ is recovered.

In abstract terms the graph shown in figure 1 is simply a second order Markov graph. This is not always the case. In Amit and Kong (1993) more complex graphs were required. Even in the present context replacing the edge between vertices 3 and 5 to an edge between vertices 3 and 6 yields comparable results, however the graph is no longer second order Markov. The match obtained for the candidate points shown in the left panel of figure 2 is shown in figure 3. For vertex 8, the

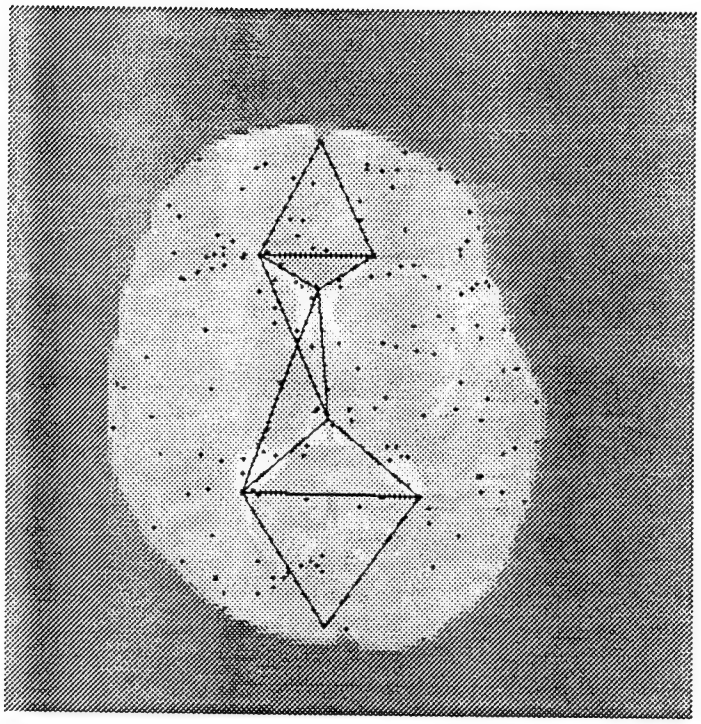

The match to the candidates in the left panel of figure 2

FIGURE 3.

algorithm prefered a candidate slightly to the left of the correct one. so not all is perfect. We address this issue in the discussion section. The match obtained for the candidate points shown on the right panel of figure 2 is shown in the left panel of figure 4 together with the match for another brain scan displayed on the right.

In figure 5 the automatic identification of anatomies obtained from the graph match is displayed.

Dynamic programming has been used in image analysis in a variety of contexts such as road tracking (Barzohar and Cooper (1993)) , stereo (Ohta and Kanade (1985)), and artery tracking (Petrocelli *et. al.* (1992)). All these settings are one dimensional in nature, and the constraints enforced by the underlying graph are all local. To our knowledge this is the first attempt to incorporate the efficient computational tool of dynamic programming in an inherently two dimensional and non-local imaging problem.

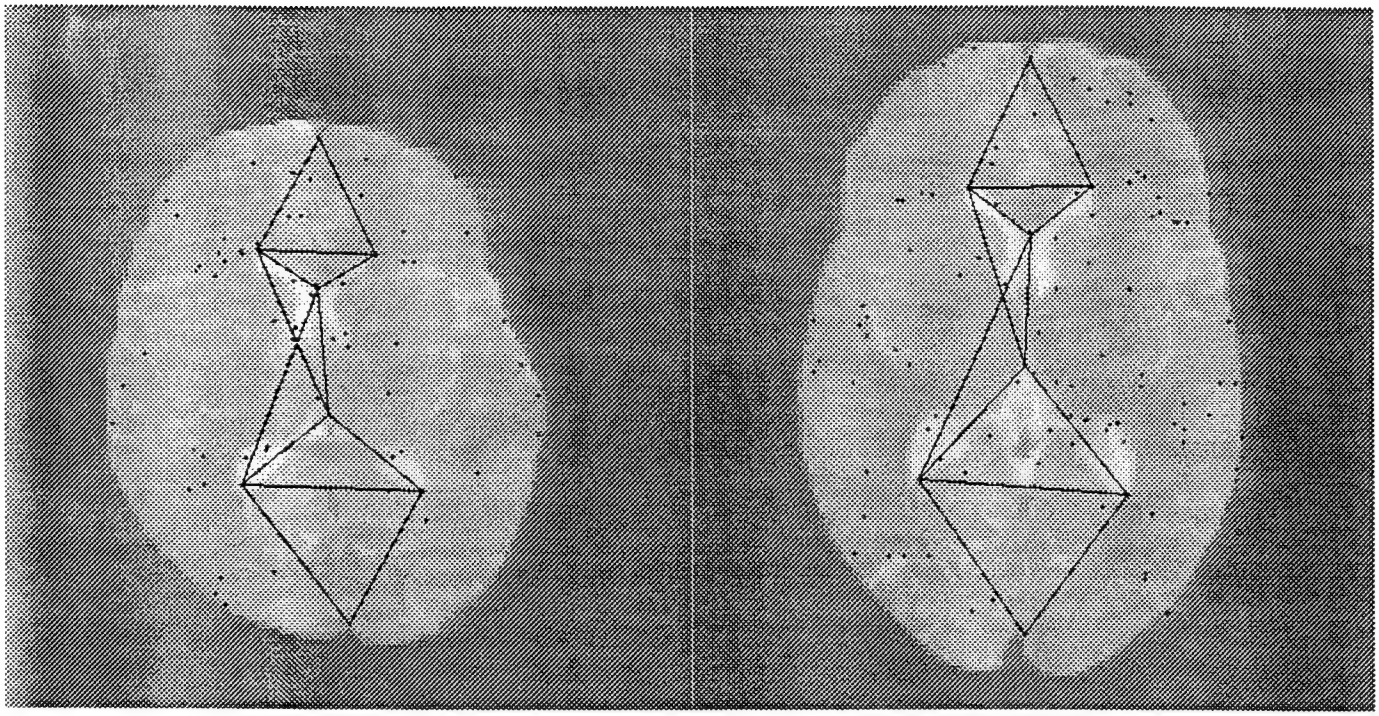

Matches for two different images, with candidates obtained with the .8 threshhold.

FIGURE 4.

Decomposability imposes certain limitations on the graph, and may limit the geometric and topological information it contains. In Amit and Kong (1993) this is addressed by starting from a non-decomposable graph which contains the desired information, splitting it into decomposable subgraphs with certain points in common. An optimal match is found using the first graph. When the optimization procedure begins for the second subgraph the match for this subset of data points is fixed as the match provided by the first subgraph. Now the optimal match is found for the remaining vertices of the second subgraph. In the problem presented here one decomposable graph was sufficient to obtain the matches.

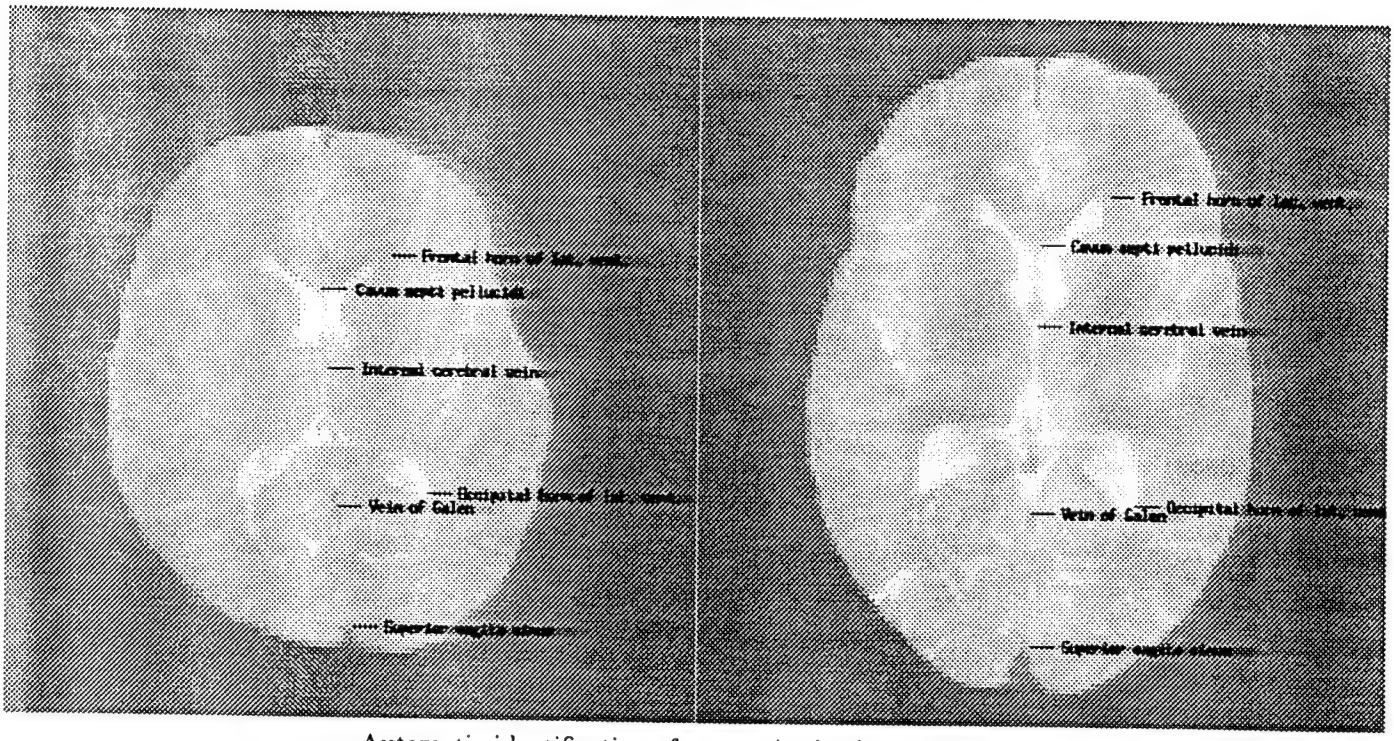

Automatic identification of anatomies in the two images.

FIGURE 5.

The cost functions

The cost function ϕ has the form

$$\begin{aligned}\phi_{ijk}(d_{\alpha_i}, d_{\alpha_j}, d_{\alpha_k}) = &\left[\log\left(l(d_{\alpha_i}, d_{\alpha_k})/l(d_{\alpha_i}, d_{\alpha_j})\right) - \log\left(l(v_i, v_k)/l(v_i, v_j)\right)\right]^2 \\ &+ \left[\log\left(l(d_{\alpha_j}, d_{\alpha_k})/l(d_{\alpha_j}, d_{\alpha_i})\right) - \log\left(l(v_j, v_k)/l(v_j, v_i)\right)\right]^2 . \\ &+ \left[\log\left(l(d_{\alpha_k}, d_{\alpha_j})/l(d_{\alpha_k}, d_{\alpha_i})\right) - \log\left(l(v_k, v_j)/l(v_k, v_i)\right)\right]^2\end{aligned}$$

where l denotes the Euclidean distance between between two points. In other words the sum of the square of the difference of the log ratios of the lengths of each pair of edges between the candidate triangle $d_{\alpha_i}, d_{\alpha_j}, d_{\alpha_k}$ and the template triangle v_i, v_j, v_k. In addition a hard constraint was imposed which did not allow an angle to change by more than $\pi/4$.

Note that these cost functions are completely scale and rotation invariant. On

the other hand the local operators although robust to large changes in scale are robust to small changes in rotation. In figure 6 we show a successful match to a rotated version ($\pi/8$) of the brain scan. Similar results were found for the other images. within a range of $(-\pi/8, \pi/8)$.

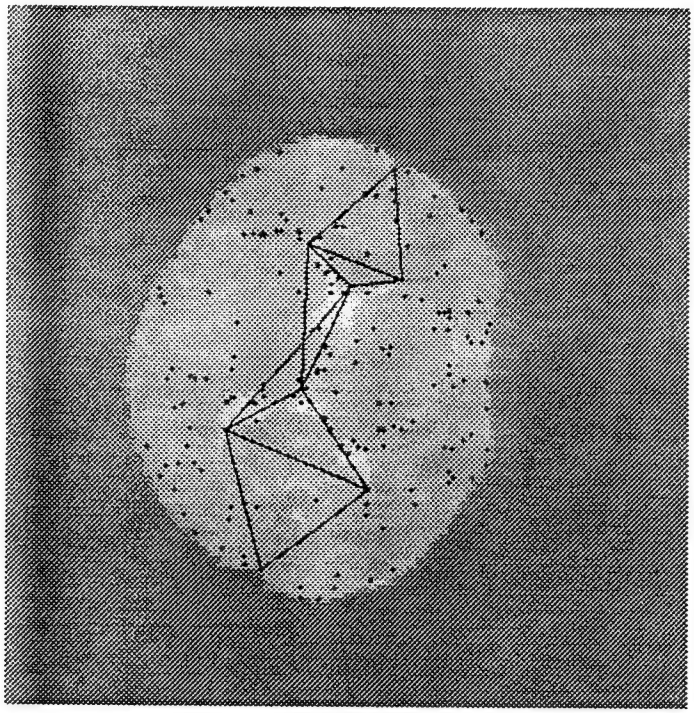

A match obtained for an image rotated by $\pi/8$.

FIGURE 6.

At $\pi/4$ the algorithm failed, the operators were completely missing the correct points. Note that a match of the graph provides the orientation of the object as a side benefit. This partial rotation invariance for a certain range of angles in the neighborhood of zero. can yield a fully rotation invariant algorithm. In the present context the image would be rotated at $0, \pi/4, \pi/2, \ldots$ and for each such angle a match would be obtained. The angle with a match of minimal cost would be used to identify the correct match and the correct orientation.

Computation

The landmarks candidates are identified in the data through some routines operated through MATLAB, and take 10-15 seconds on a SUN SPARC 10. The software for obtaining the optimal match is written in C, and also takes 10-15 seconds on the same machine with approximately 400 candidates all together for all landmarks, (about 50 per landmark). The software is available upon request.

§3 Discussion

The strength of this algorithm is its computational efficiency and the absence of any need to initialize the matching algorithm or the optimization procedure. This is one of the drawbacks of many *relaxation* techniques. If the template or model is not initially set nearby the correct location the relaxation algorithm may end up in completely erroneous solutions. This is for example the problem with the dedicated template models of Yuille *et. al.* (1989), or in Cootes and Taylor (1992b), as well as for the elastic matching models mentioned above.

The methodology presented here is new and many question remain open. At the moment the masks for the local operators are automatically obtained once the landmarks are pointed out by the user in a chosen template image. How should the thresholds be determined, should there be a score associated with each candidate according to some criterion? Such scores could be estimated using training images together with some statistic of the pixel configuration in the neighborhood of the landmark. This may help resolve local mismatches as in figure 3. How would other types of the many local operators proposed in the computer vision literature perform in conjunction with the graph models? Could different operators be used at different image resolutions to obtain matching at various levels of detail?

There remains the interesting question of how to automate the creation of the graph. It is hard to imagine a fully automated mechanism, because in many cases decomposable graphs will be insufficient. It is then necessary to iterate between decomposable subgraphs. However automatic generation of trial decomposable graphs with certain constraints or conditions should be possible to implement, thus aiding the user in developing the full graph to be used in the algorithm.

Finally the present optimization algorithm only identifies the best match. Finding the best k matches should make the procedure more robust, and is still feasible in polynomial time. An interesting problem would be how to chose from among these k best matches.

Another interesting issue is which image to use to generate the model. Can the model be improved as new images come in and are matched? For example certain parameters of the cost function could be updated to reflect the individual distributions of the triangles in the graph. Even the 'mean' triangle provided by the initial graph model may change.

References

1. Amit Y., Grenander U. and Piccioni M., 'Structural image restoration through deformable templates', Journal of the American Statistical Association, vol. 86, no. 414 pp. 376-387 (1991)

2. Amit Y., 'A non-linear variational problem for image matching', SIAM Jour. of Scientific Computing, , Vol. 15, no. 1, pp. 207-224. (1994a)

3. Amit Y. and Kong A., 'Graphical templates for image matching', Technical report no. 373, Dept. of Statistics, University of Chicago. (1994b)

4. Amit Y. and Geman D., 'Randomized Inquiries About Shape; an Application

to Handwritten Digit Recognition' Dept. of Statistics, University of Chicago. (1994)

5. Bajcsy R. and Kovacic S., 'Multiresolution Elastic Matching', Computer Vision, Graphics, and Image Processing, 46, p. 1-21, (1989).

6. Barzohar M. and Cooper D. B., 'Automatic finding of main roads in aerial images by using geometric - stochastic models and estimation', *Proc. ARPA IU Workshop Washington D. C.* (1993).

7. Bookstein L. F., *Morphometric Tools for Landmark Data : Geometry and Biology*', Cambridge University Press, Cambridge. (1991)

8. Cootes T. F., Taylor C. J. Cooper D. H., Graham J., 'Training models of shape from sets of examples', *Proceedings of BMVC* p. 9-19, (1992a)

9. Cootes T. F., Taylor C. J., 'Active shape models - Smart snakes', *Proceedings of BMVC*. p. 267-275 (1992b)

10. Grenander U., 'A unified approach to pattern analysis', in *Advances in Computers*, vol. 10. (1970)

11. Grenander U., Chow Y. and Keenan D.M., 'Hands: A Pattern Theoretical Study of Biological Shape', Research Notes in Neural Computing, vol. 2, Springer Verlag, New York. (1991)

12. Haralick R. M. and Shapiro G. L., *Computer and Robot Vision, vols. 1,2* Addison Wesley, Reading Massachusetts, (1992)

13. Horn B. K. P and Schunck B. G., 'Determining optical flow', Artificial Intelligence 17 (1981), p. 185-203.

14. Huang T. S. and Tsai R. Y., 'Image sequence Analysis: Motion estimation', in

Image Sequence Analysis, Ed. Huang T. S., Springer-Verlag, New York (1981).

15. Jin Z. and Mowforth P., 'A discrete approach to signal mapping', Technical Report TIRM-88-036, The Turing Institute, Glasgow, Scotland (1988).

16. Kass M., Witkin A. and Terzopoulos D., 'Snakes: active contour models.' International Journal of Computer Vision, vol 1, pp 321-331, (1987)

17. Mallat S., 'A theory for multiresolution signal decomposition: the wavelet representation'. IEEE Trans. Pattern Anal. and Machine Intell., 11 (1989), p. 674-693.

18. Miller M., Christensen G., Amit Y. and Grenander U., 'A mathematical textbook of deformable neuro-anatomies'. Proc. of the National Academy of Science. Vol. R90. p. 11944-11948. (1993)

19. Nagel H. H., 'Displacement Vectors Derived from Second-Order Intensity Variations in Image Sequences', Computer Vision, Graphics and Image Processing 21. p. 85-117 (1983).

20. Ohta Y. and Kanade T., 'Stereo by intra and inter scanline search using dynamic programming', IEEE PAMI vol. 7. no. 2, p. 139-154, (1985)

21. Petrocelli R. R., Elion J. L. and Manbeck M. M, 'A new method for structure recognition in unsubstracted digital angiograms', *Proceedings of Computers in Cardiology* IEEE Computer Society, p. 207-210, (1992)

22. Phillips D. B. and Smith A. F. M., 'Bayesian Faces', Technical Report TR-93-02, Department of Mathematics, Imperial College (1993).

23. Rose D. J., Tarjan R. E. and Leuker G. S., 'Algorithmic aspects of vertex elimination on graphs', Siam J. Comput., vol. 5, pp. 266-283, (1976).

24. Terzopoulos D., 'Image analysis using multigrid relaxation methods', IEEE Transactions on Pattern Anal. and Machine Intell., vol. 8, no. 2, (1988).

25. Yuille A. L., Cohen D. S., Hallinan P., 'Feature extraction from faces using deformable templates', *Proceedings CVPR* p. 104-109, (1989).